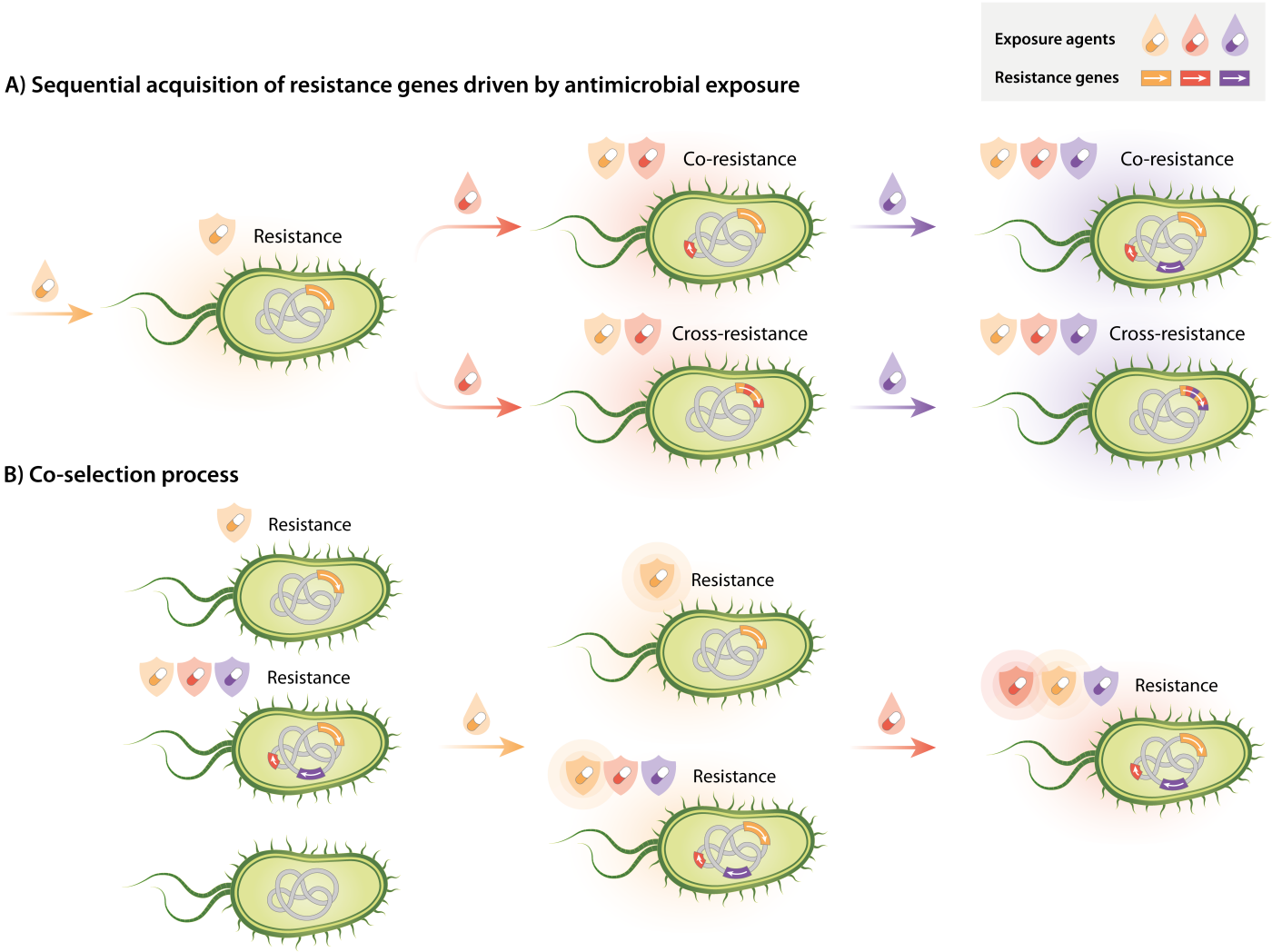

Fig S1. Emergence and co-selection of multidrug resistance in chromosomes or plasmids. A) Progressive acquisition of multiple resistances from mutations or gene transfer as a result of exposure to antimicrobial agents. Co-resistance represents the co-localization of multiple resistance genes in the same gene fragment. Cross-resistance represents a gene that confers resistance to multiple antimicrobials. B) Co-selection between multiple resistance genes upon exposure to any of the corresponding antimicrobials. This figure is adapted from the work of Cantón and Ruiz-Garbajosa [78].

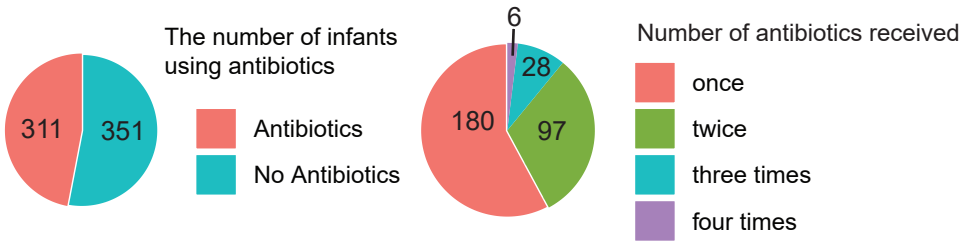

Fig S2. Summary of antibiotic usage for 662 infants during the first year.

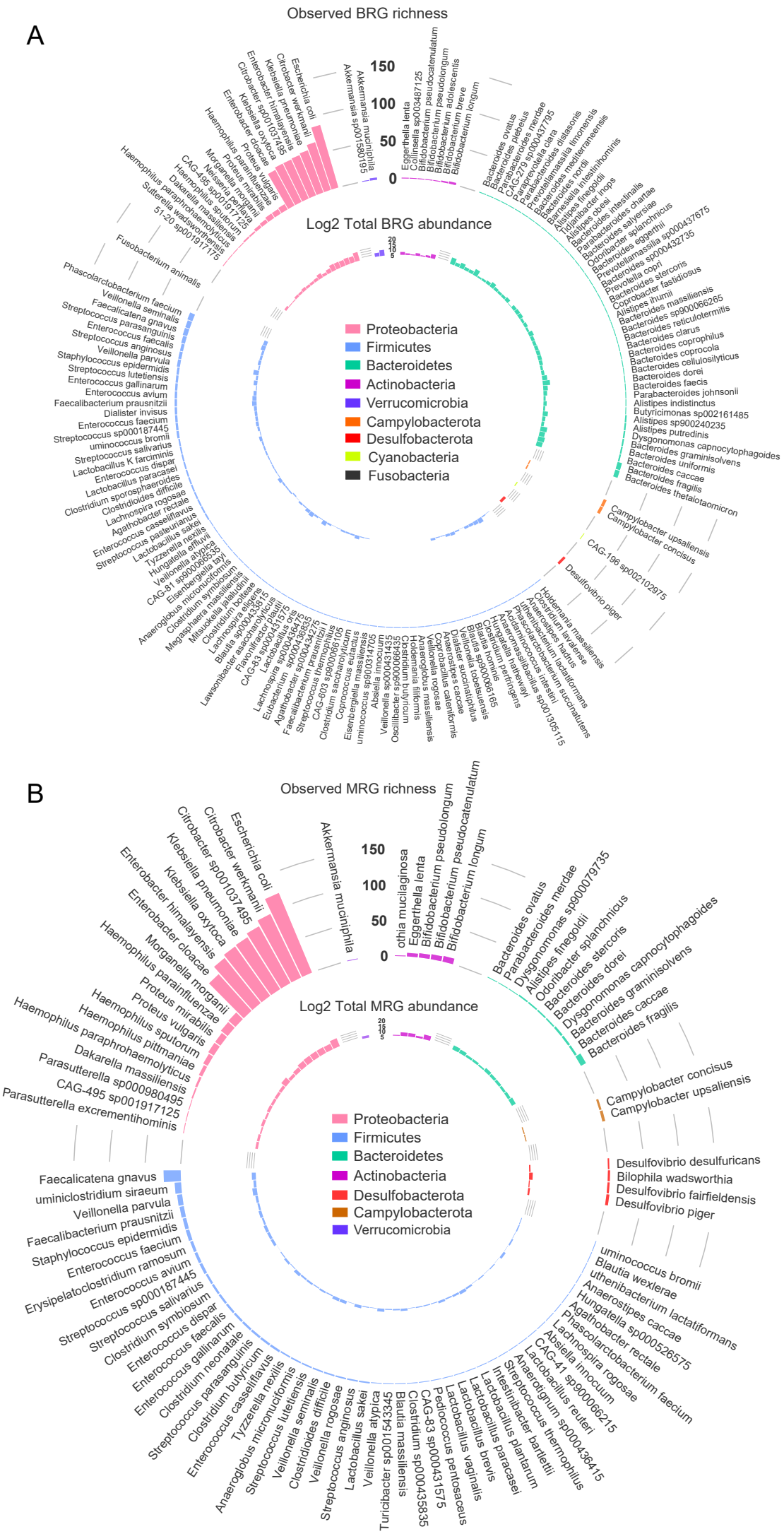

Fig S3. Distribution of gene richness and abundance among bacterial species carrying (A) BRGs, (B) MRGs, (C) virulence genes, and (D) MGEs in the infant gut.

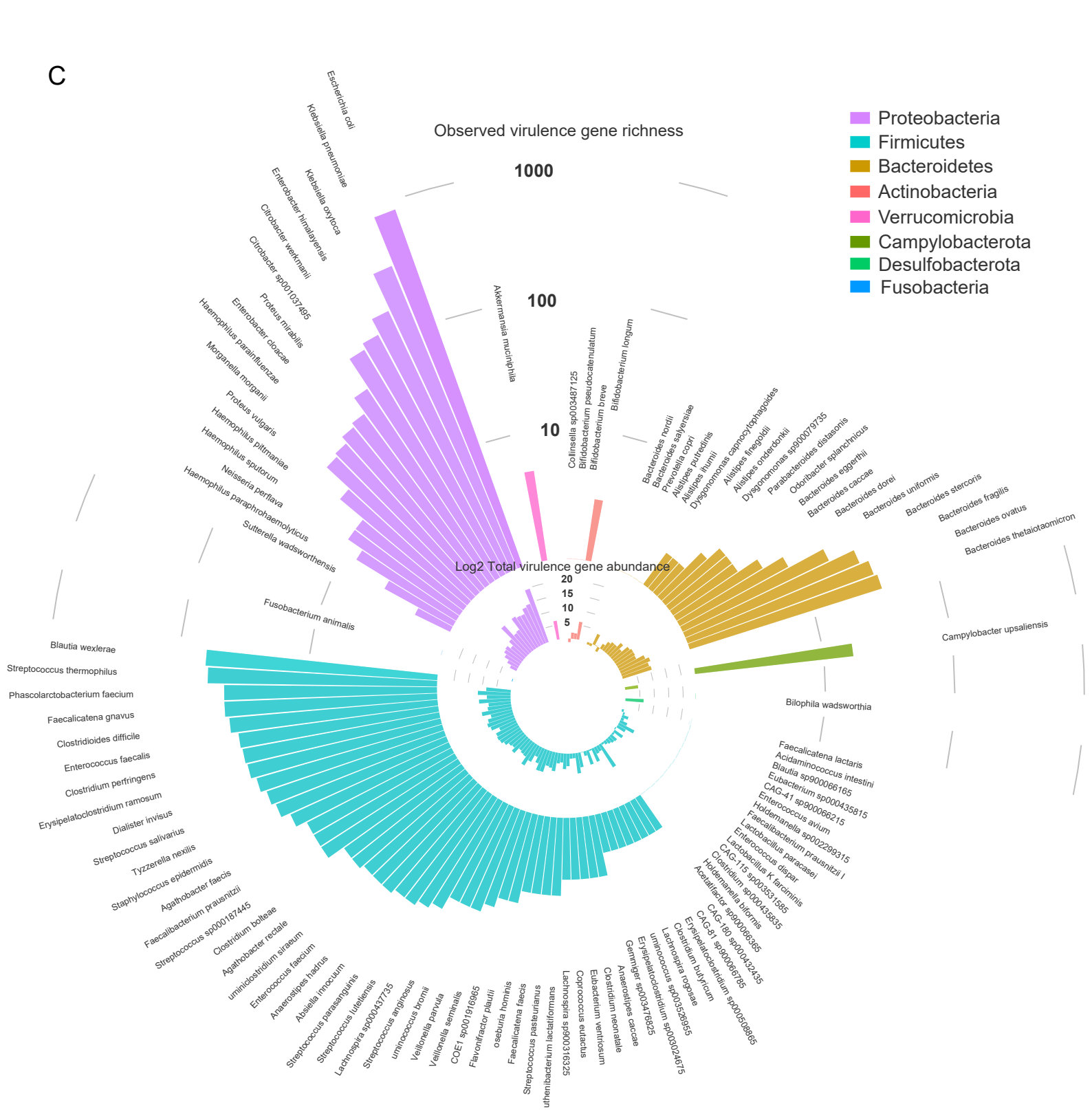
C
Observed virulence gene richness
1000
100
10
Proteobacteria
Firmicutes
Bacteroidetes
Actinobacteria
Verrucomicrobia
Campylobacterota
Desulfobacterota
Fusobacteria
Escherichia coli
Klebsiella pneumoniae
Klebsiella oxytoca
Enterobacter hormaechei
Enterobacter asburiae
Enterobacter kobei
Enterobacter roggenkampii
Enterobacter ludwigii
Enterobacter hormaechei
Enterobacter cloacae
Enterobacter asburiae
Enterobacter kobei
Enterobacter roggenkampii
Enterobacter ludwigii
Citrobacter werkmanii
Citrobacter sp001037495
Proteus mirabilis
Haemophilus parainfluenzae
Morganella morganii
Proteus vulgaris
Haemophilus pittmaniae
Haemophilus sputorum
Neisseria perflava
Haemophilus paraphrohaemolyticus
Sutterella wadsworthensis
Akkermansia muciniphila
Collinsella sp003487125
Bifidobacterium pseudocatenulatum
Bifidobacterium breve
Bifidobacterium longum
Bacteroides nordii
Bacteroides salyersiae
Prevotella copri
Alistipes putredinis
Alistipes shahii
Dysgonomonas capnocytophagoides
Alistipes finegoldii
Alistipes onderdonkii
Dysgonomonas sp900079735
Parabacteroides distasonis
Odoribacter splanchnicus
Bacteroides eggerthii
Bacteroides caccae
Bacteroides dorei
Bacteroides uniformis
Bacteroides stercoris
Bacteroides fragilis
Bacteroides ovatus
Bacteroides thetaiotaomicron
Log2 Total virulence gene abundance
20
15
10
5
Fusobacterium animalis
Campylobacter upsaliensis
Bilophila wadsworthia
Blautia wexlerae
Streptococcus thermophilus
Phascolarctobacterium faecium
Faecalicatena gnavus
Clostridioides difficile
Enterococcus faecalis
Clostridium perfringens
Erysipelatoclostridium ramosum
Dialister invisus
Streptococcus salivarius
Tyzzerella nexilis
Staphylococcus epidermidis
Agathobacter faecis
Faecalibacterium prausnitzii
Streptococcus sp000187445
Clostridium bolteae
Agathobacter rectale
uminiclostridium siraeum
Enterococcus faecium
Anaerostipes hadrus
Absiella innocuum
Streptococcus parasanguinis
Streptococcus lutetiensis
Lachnospira sp000437735
Streptococcus anginosus
uminococcus bromii
Veillonella parvula
Veillonella seminalis
COE1 sp001916965
Flavonifractor plautii
oseburia hominis
Faecalicatena faecis
Streptococcus pasteurianus
uthenibacterium lactatiformans
Lachnospira sp900316325
Coprococcus eutactus
Eubacterium ventriosum
Clostridium neonatale
Anaerostipes caccae
Gemmiger sp003476825
Erysipelatoclostridium uminococcus sp003526955
Lachnospira rogosae
Clostridium butyricum
Erysipelatoclostridium sp003024675
CAG-91 sp900066785
CAG-180 sp900043435
Erysipelatoclostridium sp900508865
Holdemanella biformis
Acetatifactor sp900066365
Clostridium sp000435835
CAG-115 sp000531585
Lactobacillus K farciminis
Enterococcus dispar
Lactobacillus paracasei
Faecalibacterium prausnitzii I
Holdemanella sp002299315
Enterococcus avium
CAG-41 sp900066215
Eubacterium sp000435815
Blautia sp900066165
Acidaminococcus intestini
Faecalicatena lactaris

D

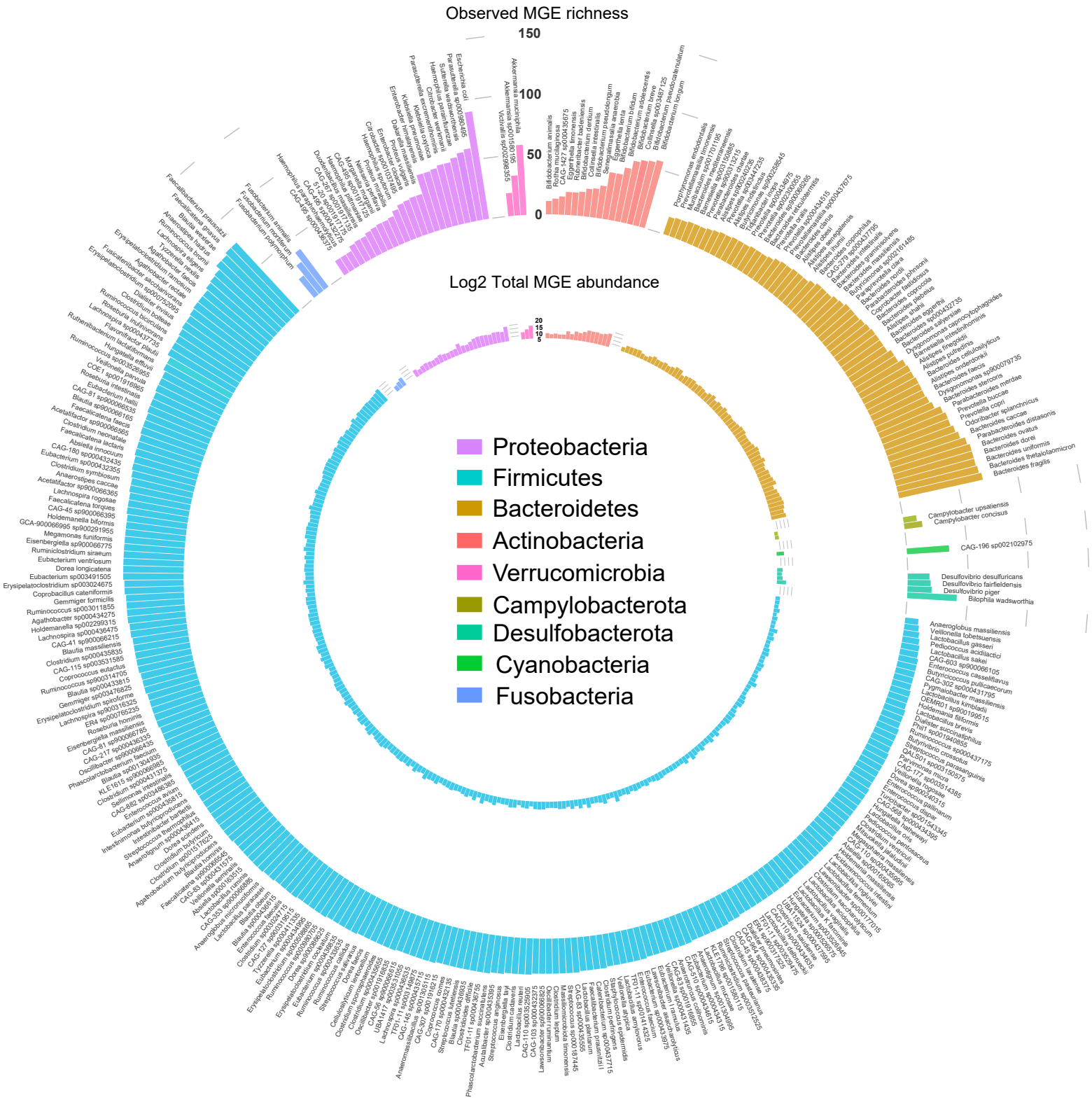
Observed MGE richness
150
100
50
0
Log2 Total MGE abundance
20
15
10
5
Proteobacteria
Firmicutes
Bacteroidetes
Actinobacteria
Verrucomicrobia
Campylobacterota
Desulfobacterota
Cyanobacteria
Fusobacteria

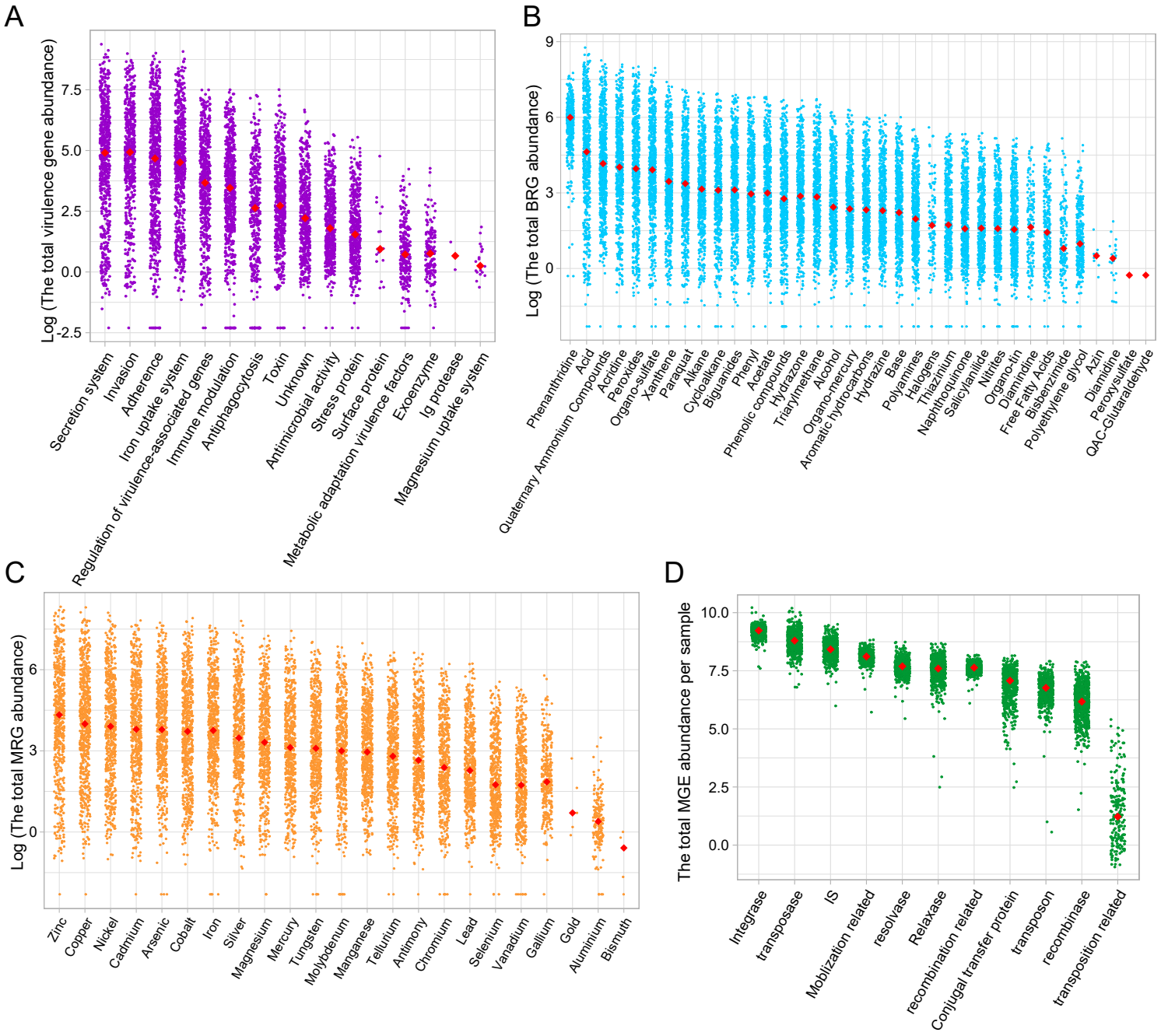

Fig S4. Total abundance (sum of GCPM) of (A) virulence genes in log scale, (B) BRGs in log scale, (C) MRGs, and (D) MGEs in log scale in the infant gut. The labels on the x-axis describe (A) virulence factors, (B) biocides, (C) metals, and (D) categories of MGEs. The red dot in the scatter plot represents the median value of the total abundance.

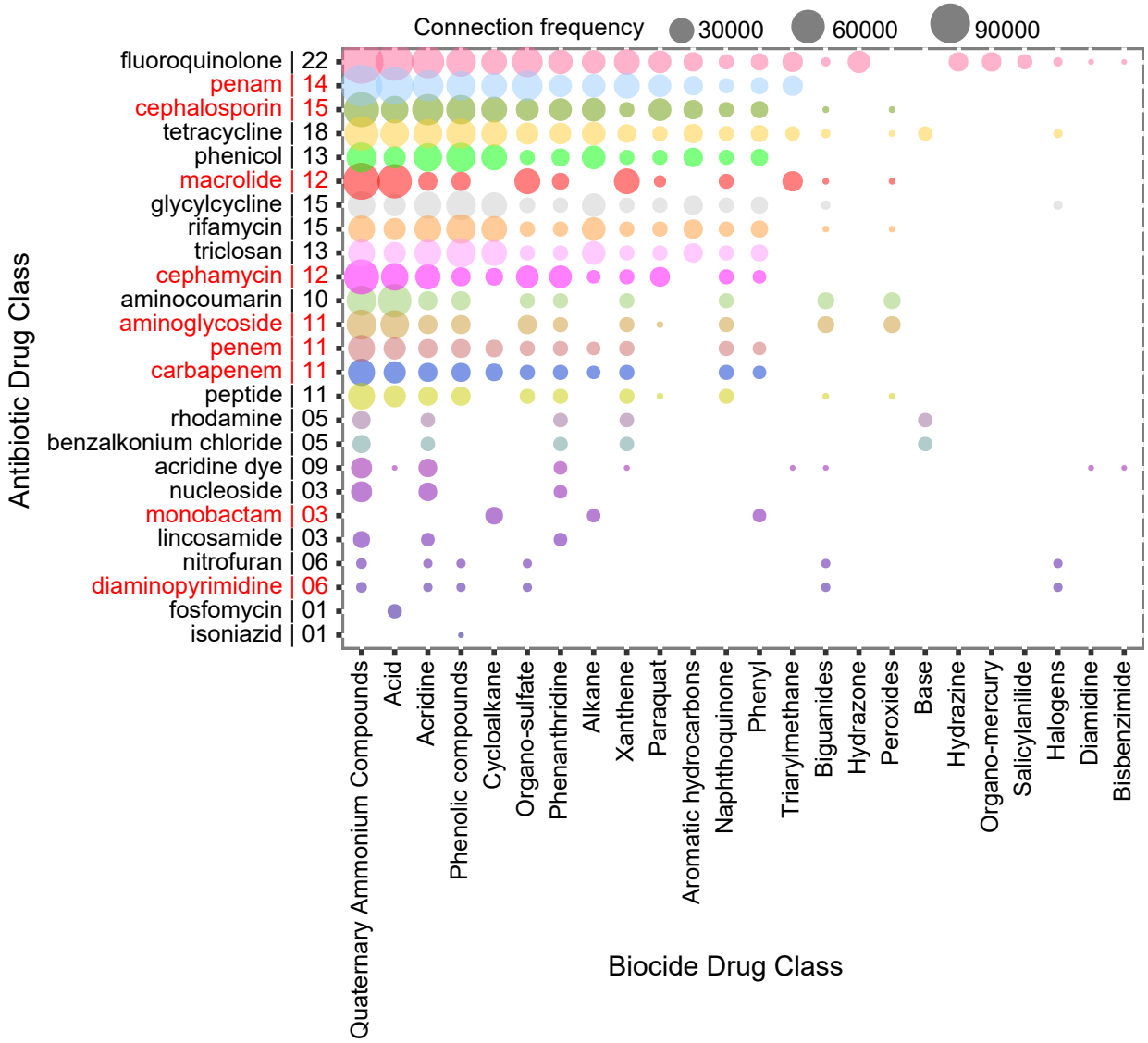

Fig S5. Co-localization bubble chart representing the drug classes related to 42 ABRGs. The size of the bubble is proportional to the abundance of the ABRGs. The drug classes in red represent those used in this cohort.

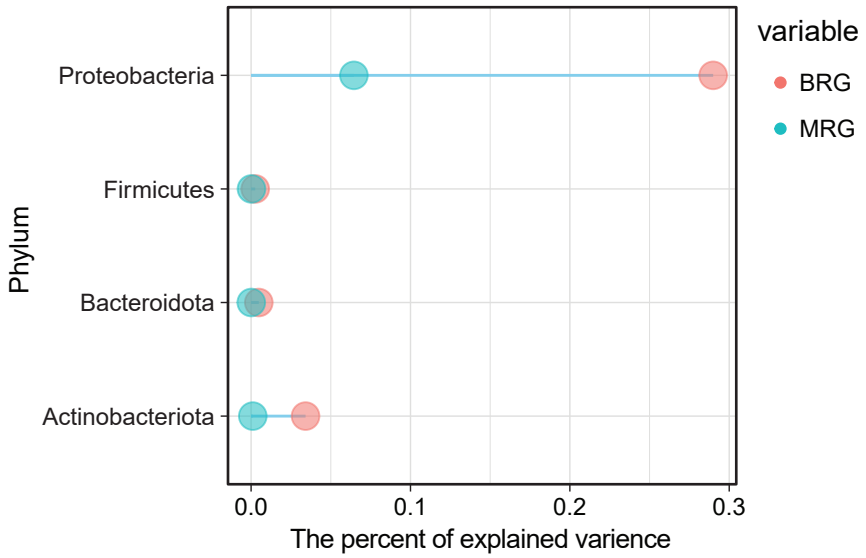

Fig S6. The pecent of varience explained by different phyla in the co-localization of ARGs and BRGs/MRGs

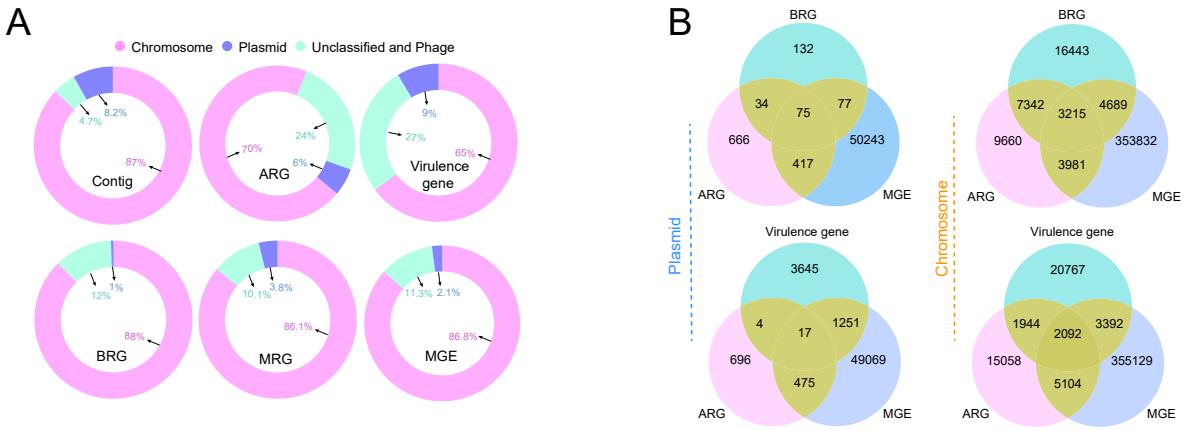

Fig S7. Distribution and Co-localization of ARGs, BRGs/VGs, and MGEs on plasmids or Chromosome in the infant gut. A) The respective abundance (percentage) of contigs, resistance genes, VGs, and mobile genetic elements in chromosomes and plasmids. B) Venn diagram depicting the number of contigs with resistance genes and MGEs in chromosomes and plasmids.

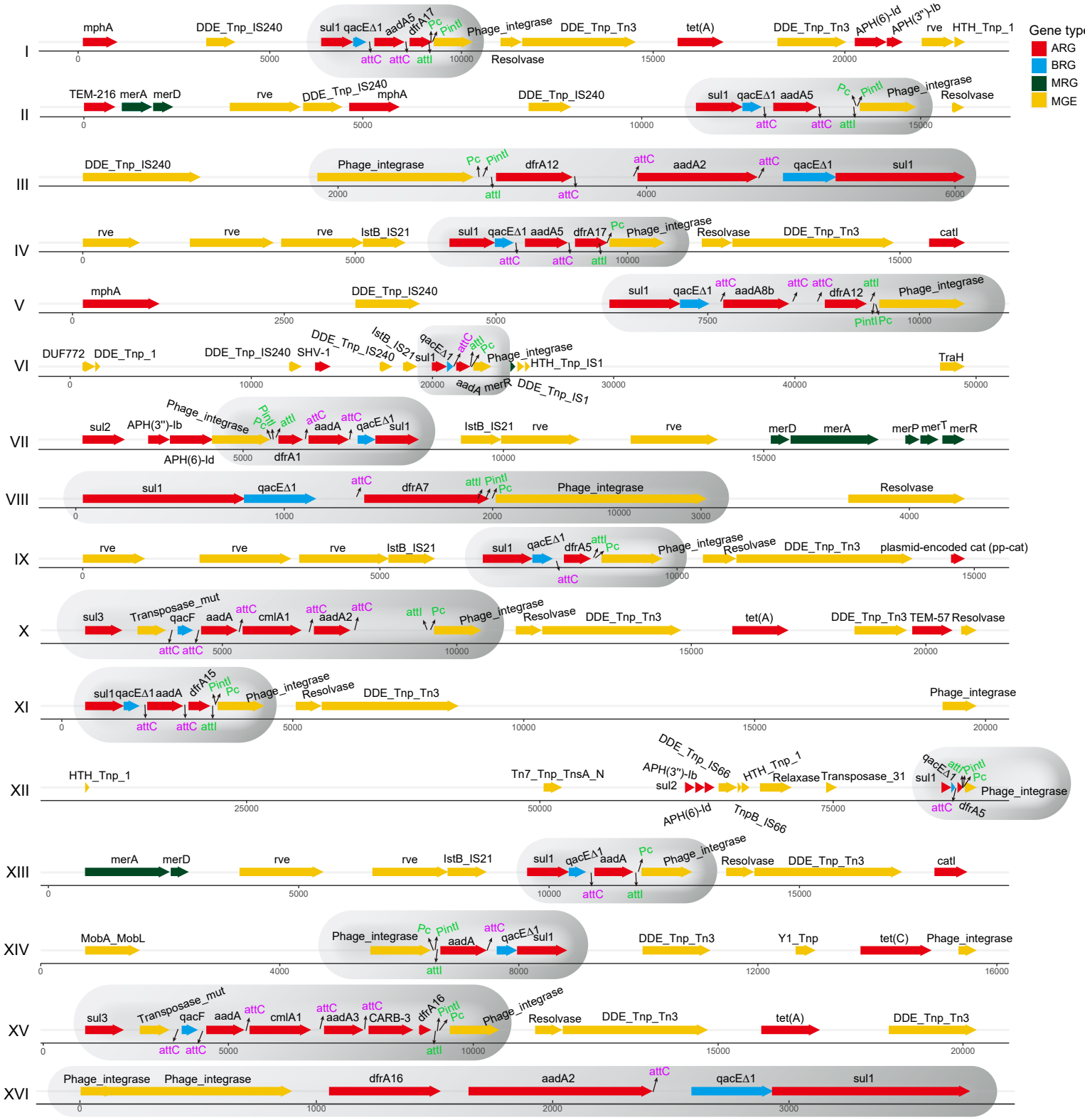

Fig S8. The representative co-localization contigs carrying the different types of integrons on plasmids. Based on the ARGs on the 22 representative contigs, 16 representative contigs carrying class 1 integrons were chosen and listed in the figure (each representative contig represents a group consisting of 1 to 16 contigs). The complete integron in each contig is highlighted in gray. For ease of viewing, we only marked the approximate location of the attC recombination site, the constitutive promoter Pc for the gene cassettes, the promoter for the integrase gene PintI, and the integration site attI. To target potential mobile ARGs, we only focused on the co-localization contigs carrying MGEs on the plasmids. The location and length of genes are proportional to the actual conditions.

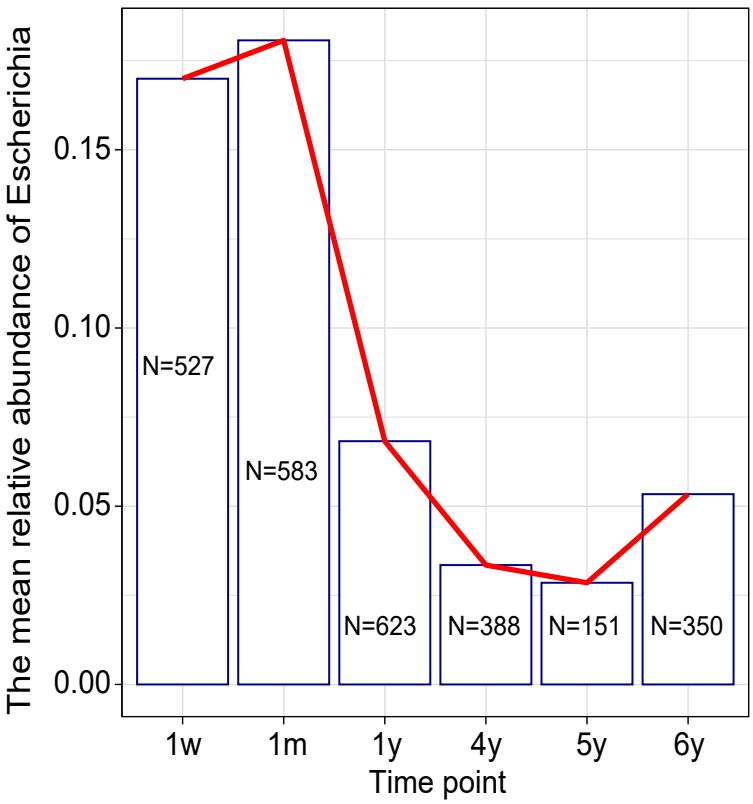

Fig S9. The mean relative abundance of E. coli in the gut of infants at one week, one month, one year, four years, five years, and six years of age based on 16S sequencing data.

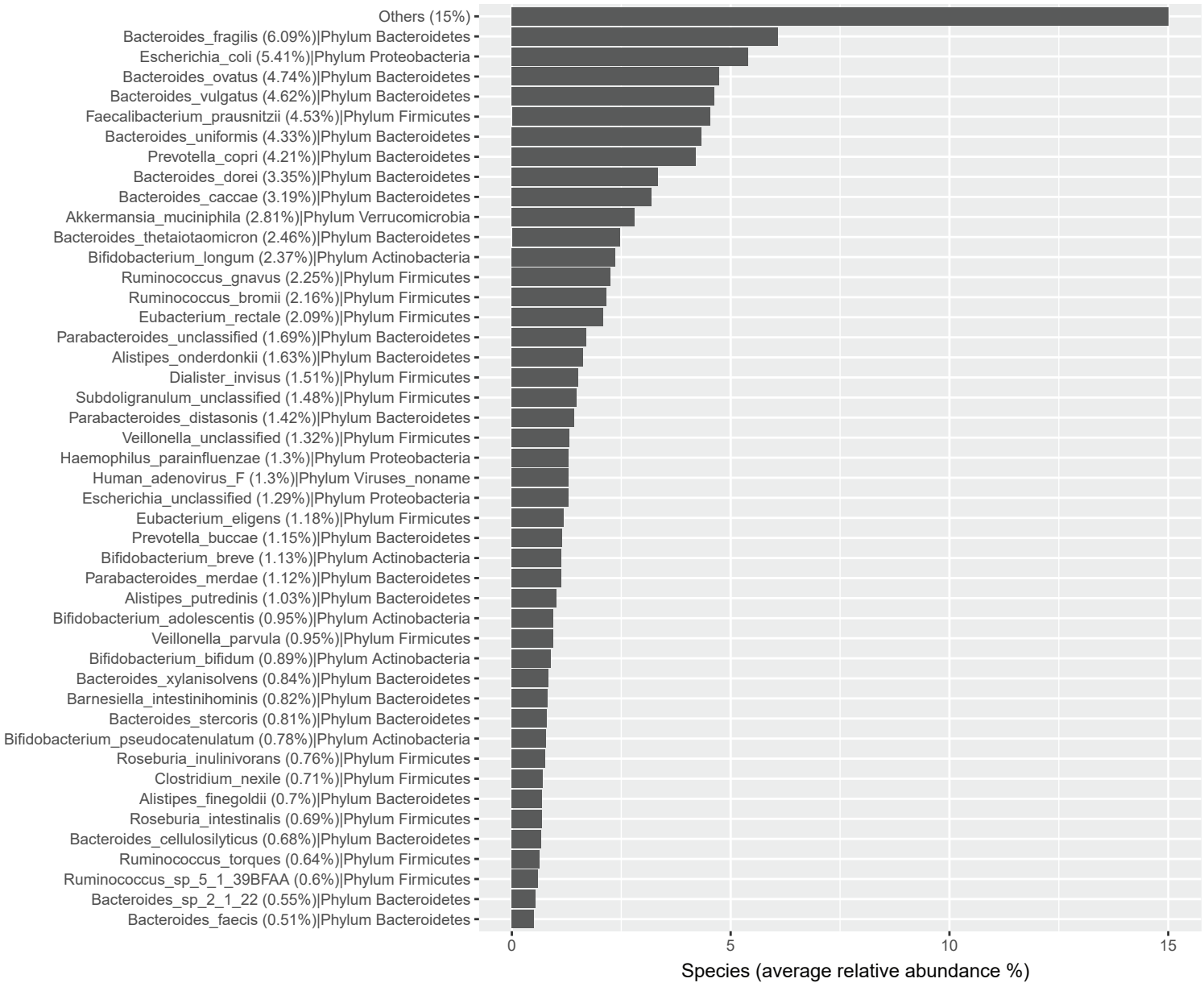

Fig S10. The percent of the 45 most abundant bacterial species in the infant gut.

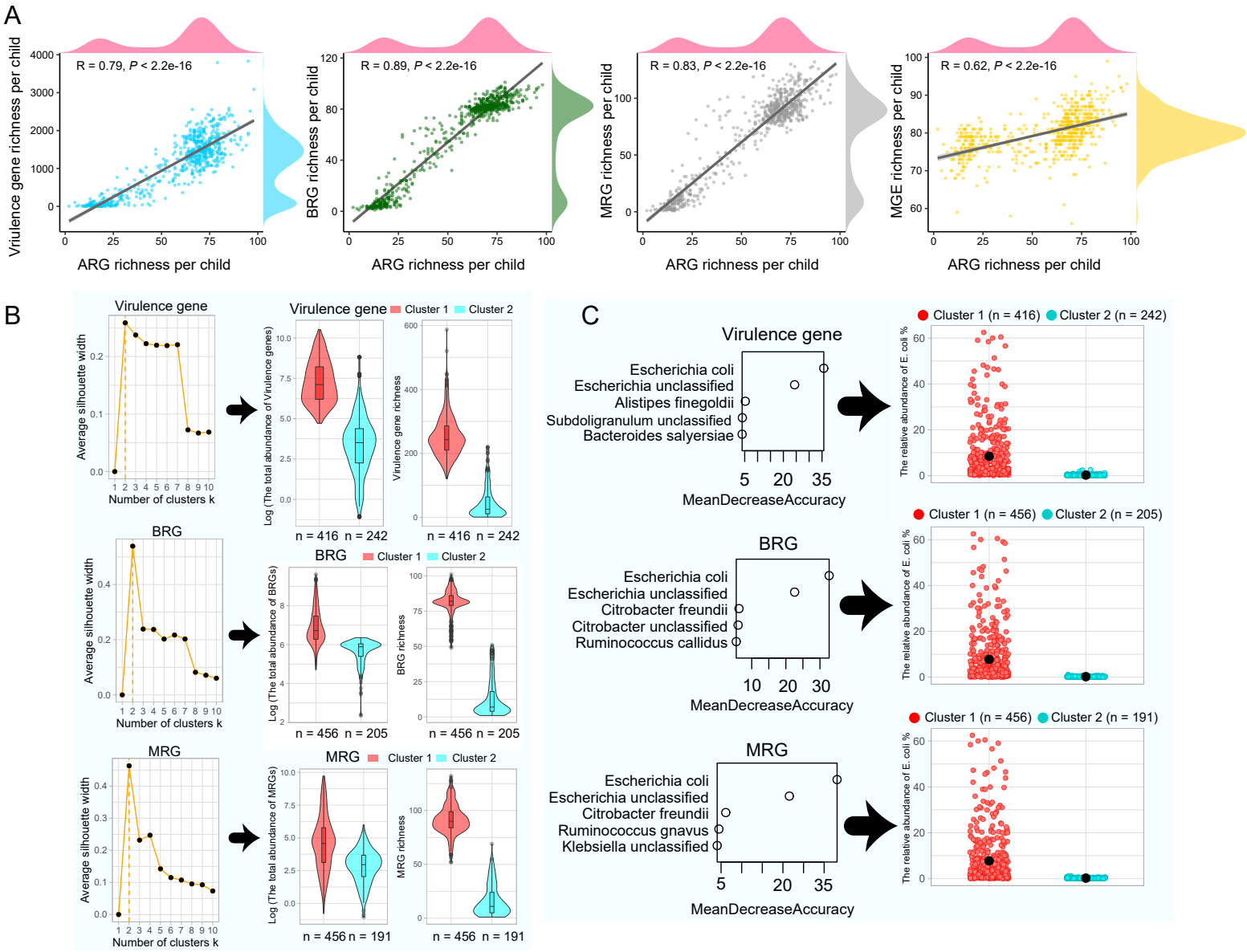

Fig S11. E. coli drives the bimodal distribution of BRGs, MRGs, and virulence genes in the infant gut. **A)** Density plot of gene richness among infants and Spearman correlation analyses between the richness of ARGs and other genes. Y-axis (not shown in the density plot) represents the number of infants. The linear regression curve and confidence interval are plotted as an illustration; inference was performed with the Spearman correlation coefficient R and the corresponding p-value ($p < 0.05$ as the significance cutoff). **B)** Average silhouette width associated with PAM clustering when different numbers of clusters were used, and the total abundance and richness of genes in the two clusters. A high average silhouette value indicates strong clustering. k = 2 was the optimal number of clusters. **C)** Importance of the top five bacterial species to the grouping of PAM clusters, as determined with a Random Forest-based approach using the mean decrease in accuracy and the relative abundance of E. coli in the two clusters. Species are ordered top-to-bottom as most-to-least important.